Brief Report

Not peer-reviewed version

Comparison of LIRADS 5 Image Guided Core Biopsy Derived From Formalin Fixed and Frozen Tissue Cores for Radiogenomics and Radioproteomics Analysis in Well, Moderate and Poorly Differentiated Hepatocellular Carcinoma

Margaret Simonian *, David sk Lu, Julian P Whitelegge, Whitaker Cohn, Preeti Ahuja, William Hsu, Steven Raman

Posted Date: 19 January 2024

doi: 10.20944/preprints202401.1491.v1

Keywords: Liver HCC, radioproteomics, radiogenomics

Brief Report

Comparison of LIRADS 5 Image Guided Core Biopsy Derived From Formalin Fixed and Frozen Tissue Cores for Radiogenomics and Radioproteomics Analysis in Well, Moderate and Poorly Differentiated Hepatocellular Carcinoma

Margaret Simonian [1,*], David S.K. Lu [1], Julian Whitelegge [2], Whitaker Cohn [2], Preeti Ahuja [1], William Hsu [1] and Steven S. Raman [1]

[1] Dept of Radiological Sciences, David Geffen School of Medicine, UCLA
[2] Semel Institute for Neuroscience & Human Behavior, Pasarow mass spectrometry lab, David Geffen School of Medicine, UCLA
* Correspondence: Margaret@chem.ucla.edu; MSimonian@mednet.ucla.edu

Abstract: The aim of this pilot study is to evaluate and compare the quality of the genomics and proteomics data obtained from paired formalin fixed paraffin embedded (FFPE) and frozen (FF) tissue percutaneous core biopsies of LIRADS 5 hepatocellular carcinoma (HCC) of varying histological grade. The preliminary data identified differentially expressed proteins and genes in poor, moderate and well differentiated HCC biopsies, with a greater efficacy in fresh frozen samples. The data offered valuable insights into the characteristics and suitability of samples for future studies.

Keywords: liver HCC; radioproteomics; radiogenomics; biomarkers

Introduction

Hepatocellular carcinoma (HCC) is the most common liver cancer and it's the leading cause of cancer-related deaths worldwide. HCC patients do not respond to most systemic therapies [1,2].

Current diagnostic tests are blood, imaging, and biopsy, with no useful predictive biomarkers. Very few proteomics biomarkers have been studied for liver HCC and their correlation to clinical behavior and response to therapy is limited [3–5]. Targeted therapy is also not available which limits the potential of personalized therapy for HCC patients. Therefore, we aim to analyze the tissue biopsies of HCC patients of different grades, using proteomics and genomics analysis, and combine it with our imaging CT/MRI data (radiomics) to generate radioproteomics and radiogenomics data to better predict HCC subtypes and ultimately offer personalized medicine for HCC patients.

Most of the tissue biopsies, in most clinics, are stored as FFPE, which is the standard method used by pathologists to make diagnosis. However, comparison studies of other type of cancer tissues, suggested that using FF tissues have advantages over FFPE, such as: proteins/ DNA/ RNA are better preserved, the variability if FF tissues are lower than FFPE tissues which can affect the data quality, and FF samples can be stored for more than 2 years with no risk of DNA/protein degradation unlike FFPE samples [6,7].

Here we report the preliminary data that we obtained by comparing three paired FFPE and FF tissue biopsies, derived from 18 G percutaneous biopsy of LIRADS 5 of three histological grades (well differentiated, moderate differentiated, and poorly differentiated) HCC on histology, to determine the most optimal tissue type for our larger study.

 doi:10.20944/preprints202401.1491.v1

Materials and Methods

RNA-seq library construction and sequencing

RNA-seq libraries of three paired FFPE and FF tissue biopsies of three histological grades were prepared with KAPA mRNA HyperPrep Kit with RiboErase (Roche). rRNA was depleted by hybridization of complementary DNA oligonucleotides, followed by treatment with RNase H and DNase. The f first strand cDNA synthesized using random priming followed by second strand synthesis converting cDNA:RNA hybrid to double-stranded cDNA (dscDNA), and incorporating dUTP into the second cDNA strand. cDNA generation is followed by end repair to generate blunt ends, A-tailing, adaptor ligation and PCR amplification.

Sequencing was performed on Illumina NovaSeq6000 for a paired end 2x50 run. Data quality check was done on Illumina SAV. Demultiplexing was performed with Illumina software. The reads were mapped by STAR 2.7.9a [8] and read counts per gene were quantified using the human genome GRCh38.104. In Partek Flow [9], read counts were normalized by CPM +1.0E-4. Differential expression of genes was measured using the gene set enrichment (GSA) algorithm in Partek Flow, generating unfiltered as well as filtered datasets. Statistical filters for differential expression were set at fold-change >2 and $p<0.01$.

Deparaffinization of FFPE Tissues

FFPE tissue scrolls were placed in Eppendorf tubes, 1 mL of 100% xylene was added for 10 minutes to deparaffinized the tissue scrolls. Centrifuged 3 times, at 16,000 x g for 3 min, supernatant was discarded. Followed by 3 mL of 100% ethanol, for 3 min, pelleted at 16,000 x g for 3 minutes. This step was repeated an additional two times. Supernatant was discarded.

Protein extraction

Fresh frozen and FFPE tissues homogenization was carried out using with12 mM sodium lauryl sarcosine, 0.5% sodium deoxycholate, and 50 mM triethyl ammonium bicarbonate TEAB, in ultrasonic cell disruptor for 20 seconds. Samples were then centrifuged at 16,000 × g for 5 minutes, supernatant was collected, heated at 95°C for 1 hour and sonicated for 5 minutes. Protein disulfides were reduced with 5 mM Tris 2-carboxyethyl phosphine, for 30 minutes at room temperature. Iodoacetamide 10mM was then added for alkylation, and incubation for 30 minutes at room temperature in dark. The protein solutions were diluted five-fold with 50 mM TEAB. Samples were then centrifuged at 16,000 x g for 5 minutes at room temperature, and supernatant was discarded, then lyophillized in a centrifugal evaporator. (Protocol modified from Simonian M. et al 2018) [10].

Protein concentrations

The total protein concentration of the samples was determined using BCA Protein Assay Kit (Pierce, Thermo Fischer Scientific). The standard curve was generated using Bovine serum albumin

TMT labelling and LC MS/MS

Proteins were digested with 20µl trypsin overnight, peptides collected and labelled via amine reactive Thermo Scientific TMT10plex Isobaric Mass Tag Labeling Reagents (per manufactures protocol), to provide multiplexed protein identification and quantitation. In brief, the reduced and alkylated proteins were transferred into TMT Reagent vials. Incubated for 1 hour in room temperature. Five% hydroxylamine was then added and incubate for 15 minutes to quench the reaction. Samples were combined at equal amounts and store at -80°C. Each 10plex experiment was fractionated via High pH Reversed-Phase Fractionation chromatography prior to LC/MS2 analysis. Peptides were injected onto a laser pulled nanobore C18 column with 1.8 um beads, then resolved using a 3-hour gradient optimized on a hybrid quadrupole-Orbitrap mass spectrometer in dd-MS2 mode (QE Plus; Thermo Fisher). The raw data were analyzed in Proteome Discoverer 2.1 for protein identifications and measurements of abundance for the identified peptides.

Preprints (www.preprints.org) | NOT PEER-REVIEWED | Posted: 19 January 2024 doi:10.20944/preprints202401.1491.v1

Results

RNA-seq identified 12,791 genes with 594 overlapping differentially expressed genes. The gene quantification efficiency of sequencing data gathered from FF was markedly higher than from FFPE tissues, with average gene counts per mapped reads of (0.61) vs (0.35) respectively (Figure 1). However, the overlapping upregulated genes in FFPE were higher than FF in the three histological grades, likely, due to tissue heat response associated with FFPE sample preparation. On histological grades comparison analysis, the overlapping upregulated genes in the moderately differentiated tissue cores were slightly higher than well differentiated tissue and markedly higher than poorly differentiated tissue cores in both FF and FFPE biopsy samples. (Figures 2 and 3).

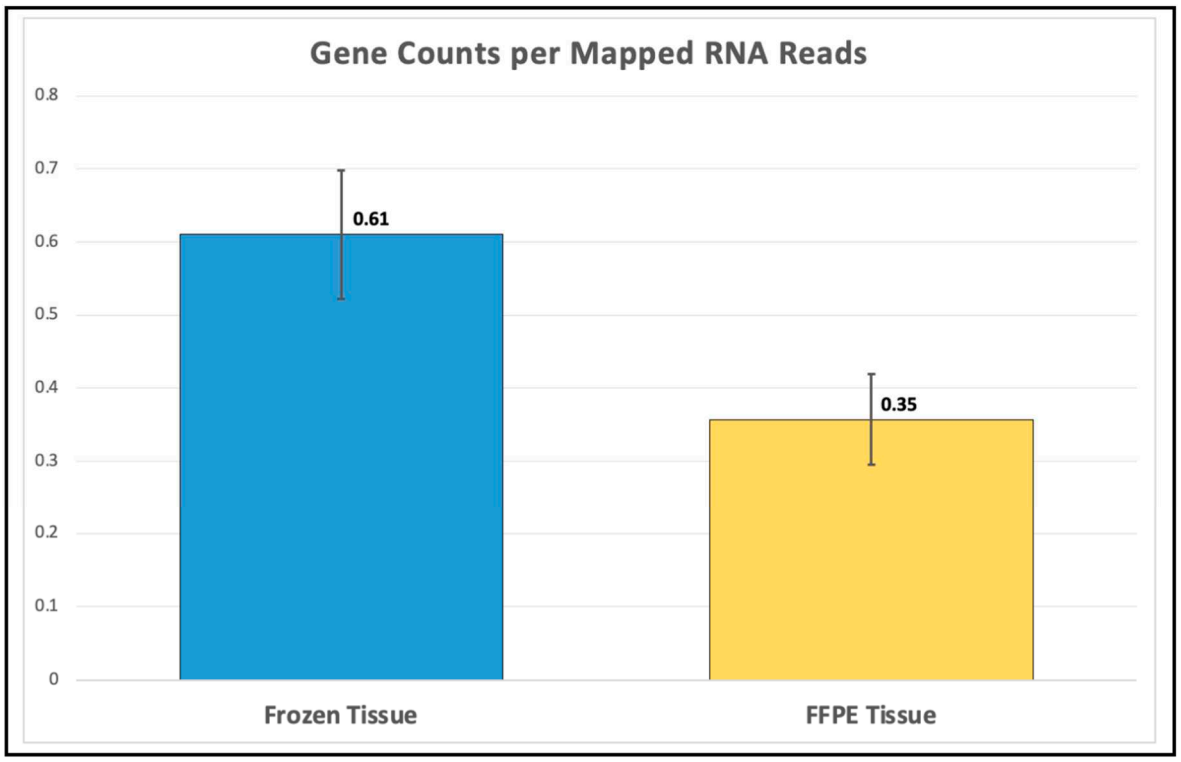

Figure 1. Higher gene counts in FF tissues over FFPE.

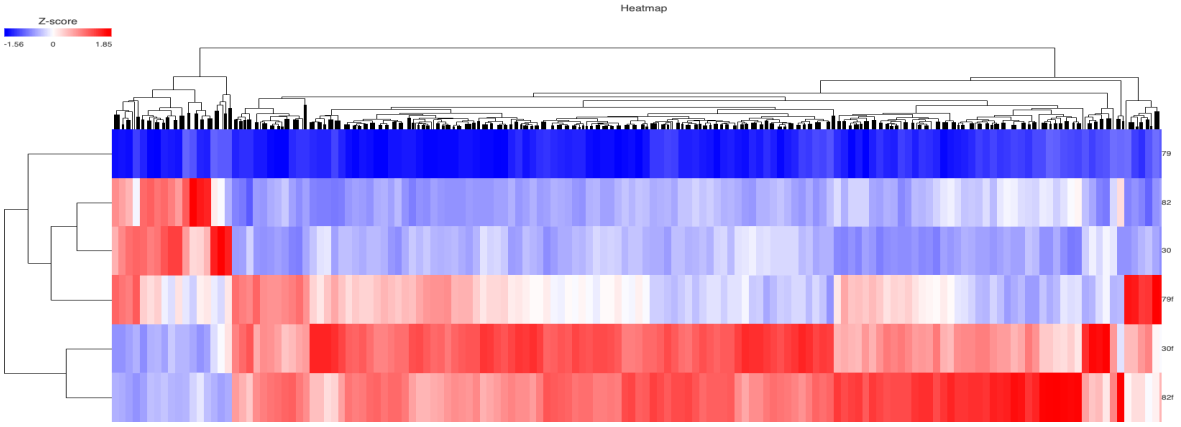

Figure 2. Heat map of overlapping genes in FFPE and FF in all phenotypes. (30= FF moderate, 30f= FFPE moderate, 82= FF well, 82f= FFPE well).

Preprints (www.preprints.org) | NOT PEER-REVIEWED | Posted: 19 January 2024 doi:10.20944/preprints202401.1491.v1

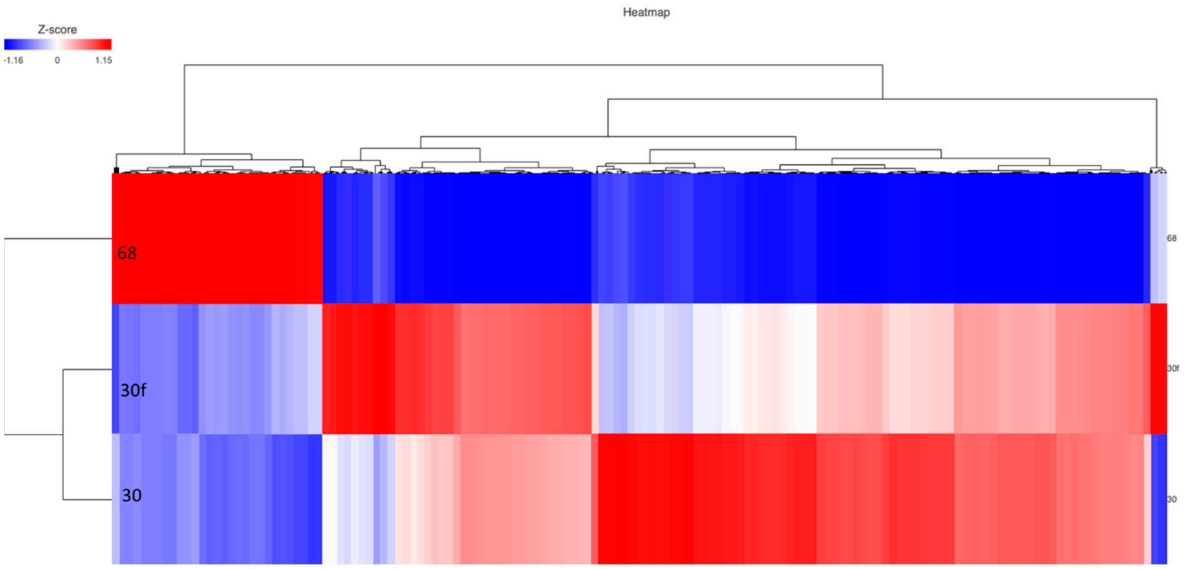

Figure 3. Heatmap of moderate vs poor in FFPE and FF. (68= poor, 30= FF moderate, 30f= FFPE moderate).

From the 594 overlapping genes, 5 genes were significantly upregulated (fold-change >2) in moderate vs well differentiated tissue cores in both FF and FFPE, with greater fold change in FF samples e.g., MBL2 expression in (moderate FF) vs (well FF) = 25-fold, while in (moderate FFPE vs (well FFPE) = 3-fold; GLUL expression in (moderate FF) vs (well FF) = 27-fold, while in (moderate FFPE vs (well FFPE) = 5-fold. (Table 1)

Table 1. The significantly upregulated genes >2 fold, in moderate vs well differentiated tissue cores in both FF and FFPE, with greater fold change in FF, due to higher gene counts.

	Frozen tissues (FF)			FFPE tissues		
Gene name	Normalized Gene Count moderate	Normalized Gene Count well	Fold-Change (moderate vs well)	Normalized Gene Count moderate	Normalized Gene Count well	Fold-Change (moderate vs well)
SCD	3280.54	101.16	32.41	1503.52	535.03	2.81
ACSL4	929.61	7.07	131.55	181.51	32.86	5.52
MBL2	392.09	15.94	24.58	194.96	65.80	2.96
RELN	596.45	24.03	24.81	293.06	81.29	3.61
GLUL	8238.2	300.55	27.41	4000.74	840.19	4.76

Additionally, 30 more genes were upregulated in moderate vs well differentiated in both FF and FFPE tissue cores, but with a fold-change <2. (Supplementary Table 1).

The proteomics data identified 466 proteins from FF and 321 proteins from FFPE, with 222 overlapping differentially expressed proteins. More upregulated proteins were identified in FF vs FFPE is all phenotypes, including in the overlapping proteins, with greater fold-change in FF, due to higher concentration of proteins in Frozen tissue (Figure 4, supplementary Table 2).

Preprints (www.preprints.org) | NOT PEER-REVIEWED | Posted: 19 January 2024 doi:10.20944/preprints202401.1491.v1

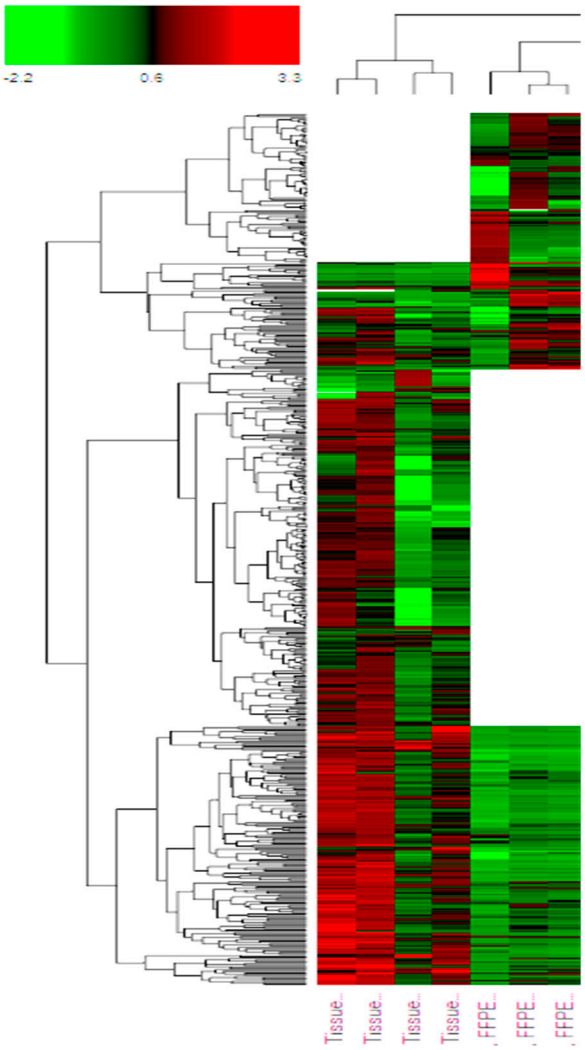

Figure 4. Heatmap of all protein identified in FF and FFPE of liver HCC from proteomics analysis.

Within overlapping proteins comparison analysis, many proteins were upregulated in moderate vs well differentiated tissue cores, in both FF and FFPE, (209 and 190 respectively), with a greater fold change in FF (Supplementary Table 2).

Additionally, 195 proteins were upregulated in poor vs moderate differentiated tissues in FF, and 214 proteins were upregulated in poor vs well differentiated tissues in FF, some of proteins are presented in Table 2, more are in supplementary Table 2.

Table 2. Some of the upregulated proteins >1 fold, in (poor vs moderate) and (poor vs well) differentiated of the frozen tissues FF.

Protein name	fold-change poor vs moderate	fold-change poor vs well
Aldehyde dehydrogenase	1.34	1.53
Profilin-1	1.01	1.23
Actin-related protein	1.15	1.11
Isoform of P0DMV9, Heat shock 70	1.12	1.12
Alpha-actinin-4	1.32	1.35
Isoform of P32754	1.10	1.72
Catalase	1.00	1.98
Adenosyl homocysteinase	1.07	1.04

 doi:10.20944/preprints202401.1491.v1

Serine hydroxymethyl transferase	1.49	1.74
Apolipoprotein A-I	1.44	1.17
Glycine amidino transferase	1.43	2.9
Myosin-9	1.02	1.06
Protein disulfide-isomerase A6	1.07	1.13
Sulfotransferase 1A1	1.22	2.27
Endoplasmin	1.18	1.03
Protein disulfide-isomerase	1.01	0.93
Isoform of P06737, Alpha-1,4	1.13	1.41

Many of the genes and proteins identified in this study play role in cancer progression, cell proliferation and immune response.

Discussion / Conclusion

The proteomics data was in agreement with the RNA-Seq data. Both FF and FFPE can be used, with higher gene and protein quantification efficacy in the FF tissue cores.

Furthermore, this study revealed the relative strengths and limitations of percutaneous biopsy derived from 18 G percutaneous LIRADS 5 HCC of varying histological grade in FFPE and FF tissues for genomics and proteomics analysis, and offered valuable insights into the characteristics and suitability of samples. Understanding these aspects is crucial for making informed decisions in the planning and execution of future experiments.

While we recognize the importance of moving to proteoform analysis, the proteogenomic analytical approach used in this pilot study was only looking at correlations with RNA data. Our future study will focus on utilizing a large number of FF biopsy tissue cores and extensive proteomics and proteoforms to significantly obtain novel biomarkers to better predict HCC subtypes and their response to therapy.

Supplementary Materials: The following supporting information can be downloaded at the website of this paper posted on Preprints.org, Table S1: Gene expression/counts in poor, moderate and well differentiated samples in FF and FFPE. Table S2: Protein abundances, and upregulation radios in in poor, moderate and well differentiated samples in both FF and FFPE.

Author Contributions: Conceptualization, Margaret Simonian, David Lu and Steven Raman; methodology, Margaret Simonian, Julian Whitelegge, Whitaker Cohn; software, Margaret Simonian, Julian Whitelegge and Whitaker Cohn; formal analysis Margaret Simonian; investigation, Margaret Simonian, David Lu, Steven Raman and Willian Hsu; resources, Steven Raman, David Lu.; data curation, Margaret Simonian.; writing—original draft preparation, Margaret Simonian; writing—review and editing, Steven Raman and Julian Whitelegge.; supervision Steven Raman, David Lu; project administration, Preeti Ahuja; funding acquisition, Steven Raman.

Funding: The study was funded in part by the UCLA Department of Radiological Sciences IDx program.

Institutional Review Board Statement: The study was performed under IRB waiver for retrospective analysis of acquired data.

Informed Consent Statement: No informed consent was obtained for retrospective analysis of acquired data.

Data Availability Statement: Data generated from this study including supplementary data, is available for viewing in this paper/journal.

Acknowledgments: The RNA-Seq analysis was conducted at UCLA Technology Center for Genomics & Bioinformatics (TCGB). Special thanks to Prof. Xinmin Li and Mark Duhon.

Conflicts of Interest: The authors declare no conflict of interest.

References

1. Galina Khemlina, Sadakatsu Ikeda, Razelle Kurzrock. 2017. The biology of Hepatocellular carcinoma: implications for genomic and immune therapies. Mol Cancer, 30;16(1):149

2. Sung H., Ferlay J., Siegel R.L., Laversanne M., Soerjomataram I., Jemal A., Bray F. 2021. Global Cancer Statistics 2020: GLOBOCAN estimates of incidence and mortality worldwide for 36 cancers in 185 countries. CA Cancer J. Clin;71(3):209–249
3. Qiang Gao, Hongwen Zhu , Liangqing Dong , Weiwei Shi , Ran Chen , Zhijian Song, et al. 2019. Integrated Proteogenomic Characterization of HBV-Related Hepatocellular Carcinoma. Cell, 3;179(2):561-577
4. Charlotte K Y Ng, Eva Dazert , Tuyana Boldanova, Mairene Coto-Llerena, Sandro Nuciforo, et al. 2022. Integrative proteogenomic characterization of hepatocellular carcinoma across etiologies and stages.Nature Communications 4;13(1):2436
5. Margaret Simonian, Angeles Baquerizo, Randolph Schaffer, et al. 2018. Analysis of differentially expressed proteins in hepatocellular carcinoma. J. Transplantation 102 : p S907. DOI: 10.1097/01.tp.0000544012.65450.1b
6. Anna Esteve-Codina, Oriol Arpi, Maria Martinez-García, Estela Pineda, Mar Mallo, et al. 2017. A Comparison of RNA-Seq Results from Paired Formalin-Fixed Paraffin-Embedded and Fresh-Frozen Glioblastoma Tissue Samples. PLoS One, 25;12(1)
7. Xian Hua Gao, Juan Li, Hai Feng Gong, Guan Yu Yu, Peng Liu, Li Qiang Hao, et al 2020. Comparison of Fresh Frozen Tissue With Formalin-Fixed Paraffin-Embedded Tissue for Mutation Analysis Using a Multi-Gene Panel in Patients With Colorectal Cancer. Front Oncol, 13:10:310
8. STAR: ultrafast universal RNA-seq aligner. A Dobin, CA Davis, F Schlesinger, J Drenkow, C Zaleski, S Jha, P Batut, M Chaisson, TR Gingeras. 2013. Bioinformatics 29 (1): 15-21.
9. Partek® Flow® software, v7.0 Copyright ©. 2019 Partek Inc., St. Louis, MO, USA.
10. Margaret Simonian, Dyna Shirasaki, Vivienne S. Lee1, David Bervini1,3, Michael Grace, et al. 2018. Proteomics identification of radiation-induced changes of membrane proteins in the rat model of arteriovenous malformation in pursuit of targets for brain AVM molecular therapy. J Clinical Proteomics, 15:43